

# Solar Neutrinos with Magnetic Moment: Rates and Global Analysis

João Pulido <sup>\*</sup>

*Centro de Física das Interacções Fundamentais (CFIF)*

*Departamento de Física, Instituto Superior Técnico*

*Av. Rovisco Pais, P-1049-001 Lisboa, Portugal*

## Abstract

A statistical analysis of the solar neutrino data is presented assuming the solar neutrino deficit to be resolved by the resonant interaction of the neutrino magnetic moment with the solar magnetic field. Four field profiles are investigated, all exhibiting a rapid increase across the bottom of the convective zone, one of them closely following the requirements from recent solar physics investigations. First a 'rates only' analysis is performed whose best fits appear to be remarkably better than all fits from oscillations. A global analysis then follows with the corresponding best fits of a comparable quality to the LMA one. Despite the fact that the resonant spin flavour precession does not predict any day/night effect, the separate SuperKamiokande day and night data are included in the analysis in order to allow for a direct comparison with oscillation scenarios. Remarkably enough, the best fit for rates and global analysis which is compatible with most astrophysical bounds on the neutrino magnetic moment is obtained from the profile which most closely follows solar physics requirements. Allowing for a peak field value of  $3 \times 10^5 G$ , it is found in this case that  $\Delta m_{21}^2 = 1.45 \times 10^{-8} eV^2$ ,  $\mu_\nu = 3.2 \times 10^{-12} \mu_B$  (65%CL). The new forthcoming experiments on solar neutrino physics (Kamland and Borexino) will be essential to ascertain whether this fact is incidental or essential.

---

<sup>\*</sup>E-mail: pulido@cfif.ist.utl.pt

# 1 Introduction

Whereas the apparent anticorrelation of the neutrino event rate with sunspot activity claimed long ago by the Homestake collaboration [1] remained unconfirmed by other experiments [2], [3], [4] and theoretical analyses [5], the magnetic moment solution to the solar neutrino problem is at present an important possibility to be explored in the quest for an explanation of the solar neutrino deficit. This is the idea, originally proposed by Cisneros [6], and later revived by Voloshin, Vysotsky and Okun [7], that a large magnetic moment of the neutrino may interact with the magnetic field of the sun, converting weakly active to sterile neutrinos. It now appears in fact that this deficit is energy dependent, in the sense that neutrinos of different energies are suppressed differently. In order to provide an energy dependent deficit, the conversion mechanism from active to nonactive neutrinos must be resonant, with the location of the critical density being determined by the neutrino energy. Thus was developed the idea of the resonance spin flavour precession (RSFP) proposed in 1988 [8]. It involves the simultaneous flip of both chirality and flavour consisting basically in the assumption that the neutrino conversion due to magnetic moment and magnetic field takes place through a resonance inside matter in much the same way as matter oscillations [9]. A sunspot activity related event rate in a particular experiment would hence imply that most of the neutrinos with energies relevant to that experiment have their resonances in the sunspot range. However, the depth of sunspots is unknown (they may not extend deeper than a few hundred kilometers) and the observed field intensity is too small in sunspots to allow for a significant conversion. The anticorrelation argument has therefore lost its appeal for several years now.

Despite the absence of the anticorrelation argument, several main reasons may be invoked to motivate RSFP and investigating its consequences for solar neutrinos. In fact both RSFP and all oscillation scenarios indicate a drop in the survival probability from the low energy (pp) to the intermediate energy neutrino sector ( $^7\text{Be}$ , CNO, pep) and a subsequent moderate rise as the energy increases further into the  $^8\text{B}$  sector. The magnetic field profiles providing good fits to the event rates from solar neutrino experiments typically show the characteristic of a sharp rise in intensity at some point in the solar interior, followed by a progressive moderate decrease [10], [11]. This is in opposite correspondence with the energy dependence of the probability in the sense that the strongest field intensities correspond to the smallest survival probabilities. Hence RSFP offers a very suggestive explanation for the general shape of the probability, which naturally appears as a consequence of the field profile. On the other hand, from solar physics and helioseismology such a sharp rise and peak field intensity is expected to occur along the tachoclyne, the region extending from the upper radiative zone to the lower convective zone, where the gradient of the angular velocity of solar matter is different from zero [12], [13]. Furthermore, it has become clear [10, 11, 14] that RSFP provides event rate fits from the solar neutrino experiments that are remarkably better than oscillation ones [15], [16]. Finally, there are recent claims in the literature for evidence of a neutrino flux histogram [17] containing two peaks, an indication

of variability pointing towards a nonzero magnetic moment of the neutrino.

This paper is divided as follows: in section 2 a statistical analysis of the four rates (Chlorine, Gallium, SuperKamiokande and SNO) on the light of the standard solar model (BP 2000) [18] and the most recent data [1, 2, 3, 4, 19] is presented. The solar neutrino deficit is assumed to be originated from nonstandard neutrinos endowed with a magnetic moment interacting with the solar magnetic field. Four solar field profiles, all obeying the general features described above, are analysed. The first three were used in a previous paper [10] at the time SNO results were non-existent. Special attention should be payed to profile (4), the one most closely following the requirements originated from solar physics investigations [13]. All Gallium measurements (SAGE, Gallex and GNO) are combined in one single data point, so that the number of d.o.f. is 2: 4 experiments - 2 parameters. These are the mass square difference between neutrino flavours  $\Delta m_{21}^2$  and  $B_0$ , the value of the field at the peak, investigated in the ranges  $(0 - 10^{-7})eV^2$  and  $(0 - 300)kG$  respectively. This  $\Delta m^2$  range is related to neutrino resonances in the region from the upper radiation zone to the solar surface, that is, the whole region where a significant magnetic field is expected. The upper bound of 300 kG for the peak field ( $B_0$ ) at the base of the convection zone is suggested by most authors [12], [13]. The neutrino magnetic moment is taken throughout at  $\mu_\nu = 10^{-11}\mu_B$ . This means that, since the order parameter is the product of  $\mu_\nu$  by the magnetic field, a suitable to fit to solar neutrino data may not allow a value of  $B_0$  well above  $10^5G$ , as it would imply a value of  $\mu_\nu$  well above  $3 \times 10^{-12}\mu_B$ , in clear conflict with astrophysical bounds on  $\mu_\nu$ . [20]. The global analysis performed in section 3 (rates + SuperKamiokande spectrum) therefore excludes all fits with  $B_0 > 10^5G$ . The border line cases (fits 2.2, 3.1 with  $B_0 = 1.18 \times 10^5G$ ,  $B_0 = 1.09 \times 10^5G$ ) were included. In order to allow for a direct comparison with the oscillation cases [15, 16, 21, 22], the day/night data from the SuperKamiokande collaboration with 1258 days [2] is included in this global analysis, despite the fact that no day/night effect is predicted by RSFP. Further, since the information on the SuperKamiokande total rate is already present in the flux of each spectral energy bin, this rate does not enter the analysis, thus following the same attitude as other authors [15, 16, 22]. The number of d.o.f. is therefore: 3 rates + 19 x 2 spectral points - 2 parameters = 39. The results are presented in terms of best fits and allowed physical region (95 %CL and 99 %CL) contours on the  $\Delta m_{21}^2$ ,  $B_0$  plane. A small discussion and conclusion section then follows.

## 2 Rates only: Chlorine, Gallium, SuperKamiokande and SNO

All profiles studied generically satisfy the requirement of a sharp rise near the bottom of the convective zone with a subsequent smoother decrease. The first three were introduced in a previous paper [10] where separate analyses of rates and spectrum were made (no global analysis) at a time when SNO results did not exist:

*Profile (1) [equilateral triangle]*

$$B = 0 \quad , \quad x < x_R \quad (1)$$

$$B = B_0 \frac{x - x_R}{x_C - x_R} , \quad x_R \leq x \leq x_C \quad (2)$$

$$B = B_0 \left[ 1 - \frac{x - x_C}{1 - x_C} \right] , \quad x_C \leq x \leq 1 \quad (3)$$

where  $x$  is the fraction of the solar radius,  $x_R = 0.70$ ,  $x_C = 0.85$  and all units are in Gauss.

*Profile (2)*

$$B = 0 \quad , \quad x < x_R \quad (4)$$

$$B = B_0 \frac{x - x_R}{x_C - x_R} , \quad x_R \leq x \leq x_C \quad (5)$$

$$B = B_0 \left[ 1 - \left( \frac{x - 0.7}{0.3} \right)^2 \right] , \quad x_C < x \leq 1 \quad (6)$$

with  $x_R = 0.65$ ,  $x_C = 0.75$ .

*Profile (3)*

$$B = 2.16 \times 10^3 \quad , \quad x \leq 0.7105 \quad (7)$$

$$B = B_1 \left[ 1 - \left( \frac{x - 0.75}{0.04} \right)^2 \right] , \quad 0.7105 < x < 0.7483 \quad (8)$$

$$B = \frac{B_0}{\cosh 30(x - 0.7483)} , \quad 0.7483 \leq x \leq 1 \quad (9)$$

with  $B_0 = 0.998B_1$ .

The fourth profile is chosen so as to more closely agree with solar physics observational requirements [13]. In fact a recent detailed study of the solar internal rotation has lead to the estimation of a large scale magnetic field. An upper limit of 300 000 G is derived for a field near the base of the convection zone, a value already claimed by previous authors [12] at this particular location. Also a field intensity of approximately 20 000 G at a depth of 30 000 km below the surface is expected. The simplest profile satisfying such features is

Profile (4)

$$B = 0 \quad , \quad x \leq x_R \quad (10)$$

$$B = B_0 \frac{x - x_R}{x_C - x_R} \quad , \quad x_R \leq x \leq x_C \quad (11)$$

$$B = B_0 + (x - x_C) \frac{2 \times 10^4 - B_0}{0.957 - x_C} \quad , \quad x_C \leq x \leq 0.957 \quad (12)$$

$$B = 2.10^4 + (x - 0.957) \frac{300 - 2 \times 10^4}{1 - 0.957} \quad , \quad 0.957 \leq x \leq 1 \quad (13)$$

with  $x_R = 0.65$ ,  $x_C = 0.713$ .

The possibility of this relatively high intensity (20 000 G) at the small depth of 30 000 km corresponding to another peak has been known for some time to be inconsistent with the data. These seem to be consistent only with a field intensity decreasing monotonically from the bottom of the convective zone to the surface [10].

The ratios of the RSFP to the SSM event rates  $R_{Ga,Cl}^{th}$  are defined as before [10], the SuperKamiokande one is

$$R_{SK}^{th} = \frac{\int_{E_{emin}}^{E_{emax}} dE_e \int_{m_e}^{\infty} dE'_e f(E'_e, E_e) \int_{E_m}^{E_M} dE \phi(E) [P(E) \frac{d\sigma_W}{dT'} + (1 - P(E)) \frac{d\bar{\sigma}_W}{dT'}]}{\int_{E_{emin}}^{E_{emax}} dE_e \int_{m_e}^{\infty} dE'_e f(E'_e, E_e) \int_{E_m}^{E_M} dE \phi(E) \frac{d\sigma_W}{dT'}} \quad (14)$$

Here  $\phi(E)$  is the SSM neutrino flux ( $hep + {}^8B$ ) and the quantity  $f(E'_e, E_e)$  is the energy resolution function [23] of the detector in terms of the physical ( $E'_e$ ) and the measured ( $E_e$ ) electron energy ( $E_e = T + m_e$ ). The lower limit of  $E_e$  is the detector threshold energy ( $E_{emin} = E_{eth}$  with  $E_{eth} = 5.0\text{MeV}$ ) and the upper limit is  $E_{emax} = 20\text{MeV}$  [2]. For the lower [10] and upper [24] integration limits of the neutrino energy, one has respectively

$$E_m = \frac{T' + \sqrt{T'^2 + 2m_e T'}}{2} \quad , \quad E_M = 15\text{MeV} \quad (i = {}^8B) \quad , \quad E_M = 18.8\text{MeV} \quad (i = hep). \quad (15)$$

The weak differential cross sections appearing in equation (17) are given by

$$\frac{d\sigma_W}{dT} = \frac{G_F^2 m_e}{2\pi} [(g_V + g_A)^2 + (g_V - g_A)^2 \left(1 - \frac{T}{E}\right)^2 - (g_V^2 - g_A^2) \frac{m_e T}{E^2}] \quad (16)$$

for  $\nu_e e$  scattering, with  $g_V = \frac{1}{2} + 2\sin^2\theta_W$ ,  $g_A = \frac{1}{2}$ . For  $\bar{\nu}_\mu e$  and  $\bar{\nu}_\tau e$  scattering,

$$\frac{d\bar{\sigma}_W}{dT} = \frac{G_F^2 m_e}{2\pi} [(g_V - g_A)^2 + (g_V + g_A)^2 \left(1 - \frac{T}{E}\right)^2 - (g_V^2 - g_A^2) \frac{m_e T}{E^2}] \quad (17)$$

with  $g_V = -\frac{1}{2} + 2\sin^2\theta_W$ ,  $g_A = -\frac{1}{2}$ .

The fourth quantity to be evaluated is the ratio of the charged current event rate by the standard charged current event rate in the SNO experiment ( $r_{CC}$ ). As recently announced

by the SNO collaboration  $r_{CC} = 0.347 \pm 0.029$  [19]. By definition  $r_{CC} = R_{CC}/R_{CC}^{st}$  where  $R_{CC}$  is given by

$$R_{CC} = \int_{T_m}^{\infty} dT_{eff} \int_Q^{\infty} dE f(E) P(E) \int_{m_e}^{E+m_e-Q} dE_e \frac{d\sigma_{CC}}{dE_e}(E, E_e) R(E_{e_{eff}}, E_e) \quad (18)$$

and  $R_{CC}^{st}$  stands for the same quantity with the replacement  $P(E) \rightarrow 1$ . In (18)  $E_{eff}$  denotes the measured total electron energy  $E_{eff} = T_{eff} + m_e$  with a threshold given in terms of the kinetic energy,  $T_m = 6.75\text{MeV}$ . The function  $R(E_{e_{eff}}, E_e)$  is the detector energy response [19] and  $Q = 1.44\text{MeV}$  with the rest of the notation being standard. The CC cross section was taken from K. Kubodera's homepage, [25].

The partial event rates for each neutrino component in each experiment were taken from [18] and the solar neutrino spectra from Bahcall's homepage [24]. The contribution of the hep flux to both the Gallium and Homestake event rates was neglected. The  $\chi^2$  analysis for the ratios of event rates and electron spectrum in SuperKamiokande was done following the standard procedure described in [10] <sup>†</sup>. The validity of this procedure and alternative ones for solar neutrinos is discussed in refs. [26], [27].

The ratios of event rates to the SSM event rates, both denoted by  $R_j^{th}$  in the following, were calculated in the parameter ranges  $\Delta m_{21}^2 = (0 - 10^{-7})\text{eV}^2$ ,  $B_0 = (0 - 30) \times 10^4\text{G}$  for all magnetic field profiles and inserted in the  $\chi^2$  definition,

$$\chi_{rates}^2 = \sum_{j_1, j_2=1}^4 (R_{j_1}^{th} - R_{j_1}^{exp}) \left[ \sigma_{rates}^2(tot) \right]_{j_1 j_2}^{-1} (R_{j_2}^{th} - R_{j_2}^{exp}) \quad (19)$$

with (Ga=1, Cl=2, SK=3, SNO=4). The measured rates  $R_j^{exp}$  in this equation can be read directly from table I. Given the four data points and the number of parameters in the fit, the number of d.o.f. is 2. Within the above parameter ranges for  $\Delta m_{21}^2$  and  $B_0$ , 19 local minima of  $\chi_{rates}^2$  were found. They are displayed in table II along with the respective values of the goodness of fit (g.o.f.). As mentioned in the introduction, a working value of  $\mu_\nu = 10^{-11}\mu_B$  was chosen. Since the order parameter is the product of the neutrino magnetic moment by the magnetic field which can be as large as  $3 \times 10^5\text{G}$  at the peak, a value  $B_0 = 10^5\text{G}$ , for example, at the local  $\chi^2$  minimum, means the existence of a solution with  $\mu_\nu = \frac{1}{3}10^{-11}\mu_B$ . In order to remain consistent with most astrophysical bounds [20], it is therefore unadvisable to consider those fits for which  $B_0$  is well above  $10^5\text{G}$ . A close inspection of table II shows that all profiles give reasonable or good quality fits for a peak field value up to  $\simeq 10^5\text{G}$ . Based on this criterion and selecting therefore fits 1.1, 1.2, 2.1, 2.2, 3.1, 4.1 (g.o.f. 34, 34, 38, 25, 42, 51% respectively) it is seen that one obtains comparable fits in RSFP to those in the oscillation cases[15, 16, 22]. In fact the best oscillation solution from the 'rates-only' analysis is the VAC one [15] for which the g.o.f. is 52%. <sup>‡</sup> Interestingly enough, the best

---

<sup>†</sup>Here only the main definitions and differences are registered. For the calculational details we refer the reader to ref.[10].

<sup>‡</sup>There is however a minor difference in criterion, since these authors considered the SAGE and Gallex/GNO rates as two separate ones, hence 3 d.o.f. in their analysis (see table 4 of ref. [15]).

of all fits investigated here is 4.1 from profile 4, the one in the closest agreement with solar physics observational requirements [13]. Whether this remarkable fact is coincidental or essential is of course too early to ascertain.

A global analysis of the selected fits 1.1, 1.2, 2.1, 2.2, 3.1 and 4.1 will now be performed in section 4.

### 3 Global Analysis

In addition to the rates, the quantity to be investigated now is the SuperKamiokande spectrum

$$R_j^{th} = \frac{\sum_i \int_{E_{ej}}^{E_{ej+1}} dE_e \int_{m_e}^{\infty} dE'_e f(E'_e, E_e) \int_{E_m}^{E_M} dE f_i \phi_i(E) [P(E) \frac{d\sigma_W}{dT'} + (1 - P(E)) \frac{d\sigma_{\bar{W}}}{dT'}]}{\sum_i \int_{E_{ej}}^{E_{ej+1}} dE_e \int_{m_e}^{\infty} dE'_e f(E'_e, E_e) \int_{E_m}^{E_M} dE \phi_i(E) \frac{d\sigma_W}{dT'}} \quad (20)$$

with  $j = 1, 38$ . Following other authors [15, 16, 22] and since the information on the SuperKamiokande total rate is already included in the flux of each spectral energy bin, this rate will now be disregarded. In order to allow for a straight comparison with other solar neutrino physics analyses the day/night spectrum is also included although no day/night difference is predicted by RSFP. Hence the  $\chi^2$  definition is as follows

$$\chi_{sp}^2 = \sum_{j_1, j_2=1}^{38} (R_{j_1}^{th} - R_{j_1}^{exp}) [\sigma_{sp}^2(tot)]_{j_1, j_2}^{-1} (R_{j_2}^{th} - R_{j_2}^{exp}). \quad (21)$$

The measured rates  $R_j^{exp}$  ( $j = 1, \dots, 38$ ) in this equation can be directly read from table II of ref. [2]. In performing the global fit one has 41 experiments (3 rates and 38 spectral data) and two free parameters, namely the mass squared difference between neutrino flavours  $\Delta m_{21}^2$  and the peak field value  $B_0$ , hence 39 d.o.f.. For the global  $\chi^2$ ,

$$\chi_{gl}^2 = \chi_{rates}^2 + \chi_{spectrum}^2. \quad (22)$$

The local minima of  $\chi_{gl}^2$  were investigated for each of the selected four fits from the previous section (1.1, 1.2, 2.1, 2.2, 3.1, 4.1). The allowed physical regions and stability of these fits were next investigated. The analysis proceeds in terms of the two parameters  $\Delta m_{21}^2$ ,  $B_0$  hence two degrees of freedom, and the results are presented in terms of 95 and 99%CL contours ( $\Delta\chi^2=5.99$  and 9.21 relative to the local best fit). Global fits 1.1 and 1.2 of profile 1, whose contours merge, and 3.1 of profile 3 are shown together in fig. 1. Global fits 2.1, 2.2 of profile 2, whose contours also merge, are shown in fig. 2, while 4.1 of profile 4 and its contours is shown in fig. 3. In table III the parameter values for each of these global fits including the values of  $\chi^2$  and the g.o.f. are also shown. It is seen that all g.o.f. are of the same order, with fit 4.1 being, interestingly enough, the best, although by a narrow margin. Comparing with the best global fit from oscillations (LMA solution)

[15, 16], the g.o.f. of fit 4.1 is similar but slightly smaller (64.7% compared to 67% with fixed hep flux) or reasonably smaller (compared to 85% with free hep flux). Since the hep flux was considered fixed in the present analysis, only the first comparison should be held as valid. Owing to the small and probably not physically meaningful day/night effect ( $1.29\sigma$ ) observed in the SuperKamiokande [2], spectrum and since RSFP predicts no such effect, it is to be expected that global fits in RSFP could be marginally worse, although of comparable quality. The energy spectrum corresponding to global fit 4.1 is shown in fig. 4 superimposed on the SuperKamiokande data. Allowing for a peak field value  $B_0 = 3 \times 10^5 G$ , the respective value of the magnetic moment, as seen from table III, is  $\mu_\nu = 3.2 \times 10^{-12} \mu_B$  with  $\Delta m_{21}^2 = 1.45 \times 10^{-8} eV^2$ .

## 4 Concluding Remarks

The analysis of prospects for the magnetic moment solution to the solar neutrino problem reveals both rate and global fits of reasonable or good quality. Previous analyses on RSFP [10, 11, 14], unambiguously indicated from the part of the data on rates a preference for solar field profiles with a steep rise across the bottom of the convection zone in which vicinity they reach a maximum, followed by a more moderate decrease up to the solar surface. They showed a quality of rate fits alone which is not shared by the oscillation rate fits [15]. Interestingly enough, this class of profiles is the most consistent one with solar physics and helioseismology [12, 13]. A further profile (4) was introduced in the present paper which is the simplest most closely following the present requirements from solar physics [13]. It is important to note that, as found in the present paper, this is the profile giving the best of all RSFP fits, both for the rates and global. For this (global) fit one finds that  $\Delta m_{21}^2 = 1.45 \times 10^{-8} eV^2$  and  $\mu_\nu = 3.2 \times 10^{-12} \mu_B$ , (g.o.f. 64.7%) if one allows for a solar field at the bottom of the convective zone  $B_0 = 300\,000 G$ . An analysis of spin flavour precession, both resonant and non-resonant, was also performed in a recent paper [28], whose authors limit themselves to a 'rates-only' analysis with a single profile. They find a better g.o.f. for the resonant (39%) than for the non-resonant case (28%), however substantially smaller than the best one obtained here with profile 4.

The forthcoming neutrino experiments Borexino [29] and Kamland [30] will be crucial to test the validity of the RSFP hypothesis against oscillations. In fact, at the present stage both the LMA and RSFP solutions give global fits of equally good quality and, as far as rates only are concerned, RSFP solutions provide the best of all fits. Furthermore, owing to the typical shape of the RSFP survival probability [10], which is quite different from the LMA, LOW and VAC ones at the intermediate energies [31], the RSFP solution predicts for Borexino a clearly smaller neutrino-electron scattering [32] event rate than these three oscillation solutions whose prediction is essentially the same [16]. It is quite likely that the Kamland experiment will either bring confirmation of the LMA scenario, or either disprove it, along with the less favoured solutions, LOW and VAC [16]. Consequently, in case these

are excluded by Kamland, the expectation for Borexino will naturally be that of a strong reduction relative to the standard event rate, therefore providing evidence for RSFP, unless a clear day/night effect is observed.

In the present analysis only time averaged data were considered and a fitting was made to a time constant profile 'buried' in the solar interior. If, on the contrary, the active neutrino flux turns out to be time dependent, a situation most likely to be interpreted through the magnetic moment solution with a time dependent interior field, the present approach is obviously inadequate. Averaging the event rates over time implies disregarding possible information in the data which otherwise is available if different periods of time are considered [17]. The robustness of such a procedure will greatly improve with the accumulation of more data.

## References

- [1] Homestake Collaboration: B. T. Cleveland *et al.*, *Astrophys. J.* **496**, 505 (1998); B. T. Cleveland *et al.*, *Nucl. Phys. B* (Proc. Suppl.) **38**, 47 (1995); R. Davis, *Prog. Part. Nucl. Phys.* **32**, 13 (1994).
- [2] SuperKamiokande Collaboration: S. Fukuda *et al.*, *Phys. Rev. Lett.* **86** 5651 (2001), hep-ex/0103032.
- [3] SAGE Collaboration: V. Gavrin, in Neutrino 2000, Proc. of the XIX Int. Conf. on Neutrino Physics and Astrophysics, 16-21 June 2000, eds. J. Law, R. W. Ollerhead and J. J. Simpson, *Nucl. Phys. Proc. Suppl.* **B91** 99 (2001).
- [4] Gallex+GNO Collaboration: E. Bellotti, in Neutrino 2000.
- [5] G. Walther, *Phys. Rev. Lett.* **79** 4522 (1998).
- [6] A. Cisneros, *Astrophys. Space Sci.* **10** 87 (1971).
- [7] M. B. Voloshin, M. I. Vysotsky, L. B. Okun, *Soviet J. of Nucl. Phys.* **44** 440 (1986); M. B. Voloshin, M. I. Vysotsky, *Soviet J. of Nucl. Phys.* **44** 544 (1986).
- [8] C. S. Lim and W. J. Marciano, *Phys. Rev. D* **37** 1368 (1988); E. Kh. Akhmedov, *Sov. J. Nucl. Phys.* **48** 382 (1988); E. Kh. Akhmedov, *Phys. Lett. B* **213** 64 (1988).
- [9] L. Wolfenstein, *Phys. Rev. D* **17** 2369 (1978); **20** 2634 (1979); S. P. Mikheyev and A. Smirnov, *Sov. J. Nucl. Phys.* **42** 913 (1985).
- [10] J. Pulido, E. Kh. Akhmedov, *Astropart. Phys.* **13** 227 (2000).
- [11] O. G. Miranda, C. Peña Garay, T. I. Rashba, V. B. Semikoz, J. W. F. Valle, *Nucl. Phys. B* **595** 360 (2001), hep-ph/0005259.

- [12] E. N. Parker in "The Structure of the Sun", Proc. of the VI Canary Islands School, Ed. Roca Cortes and F. Sanchez, Cambridge University Press 1996 p. 299.
- [13] H. M. Antia, S. M. Chitre, M. J. Thompson, astro-ph/0005587, to be published in *Astron. and Astrophys.*
- [14] M. Guzzo and H. Nunokawa, *Astropart. Phys.* **12** 87 (1999), hep-ph/9810408.
- [15] P. I. Krastev and A. Yu. Smirnov, hep-ph/0108177.
- [16] J. N. Bahcall, M. C. Gonzalez-Garcia and C. Peña-Garay, hep-ph/0111150.
- [17] J. Scargle and P. Sturrock, *Ap J* **550** L101 (2001), astro-ph/0011228.
- [18] J. N. Bahcall, M. H. Pinsonneault, S. Basu, *Ap. J.* **555** 990 (2001), astro-ph/0010346.
- [19] SNO collaboration: Q. R. Ahmad *et al.* *Phys. Rev. Lett.* **87** 071301 (2001).
- [20] S. I. Blinnikov, Institute for Theoretical and Experimental Physics Report No. ITEP-88-19 (1988), unpublished; S. I. Blinnikov, V.S. Imshennik, D.K. Nadyozhin, Sov. Sci. Rev. **E** *Astrophys. Space Sci.* **6**, 185 (1987); G.G. Raffelt, *Phys. Rev. Lett.* **64** (1990) 2856; *Astrophys. J.* **365** (1990) 559; V. Castellani and S. Degl'Innocenti, *Astrophys. J.* **402**, 574 (1993).
- [21] J. N. Bahcall, P. I. Krastev and A. Yu. Smirnov *JHEP* **0105** 015 (2001), hep-ph/0103179.
- [22] J. N. Bahcall, M.C. Gonzalez-Garcia, C. Peña-Garay, *JHEP* **0108** 014 (2001), hep-ph/0106258.
- [23] SuperKamiokande Collaboration, Y. Fukuda *et al.*, *Phys. Rev. Lett.* **81** 1158 (1998); Erratum-*ibid.* **81** 4279 (1998).
- [24] J. N. Bahcall's homepage, <http://www.sns.ias.edu/~jnb/>.
- [25] K. Kubodera's homepage, <http://nuc003.psc.sc.edu/~kubodera/>.
- [26] M. V. Garzelli and C. Giunti, Proc. of NOW2000, *Nucl. Phys. B* (Proc. Suppl.) **100** (2001) p.77; *ibid.*, hep-ph/0007155.
- [27] P. Creminelli, G. Signorelli and Allesandro Strumia, *JHEP* **0105** 052 (2001), hep-ph/0102234.
- [28] O. G. Miranda, C. Peña-Garay, T. I. Rashba, V. B. Semikoz and J. W. F. Valle, *Phys. Lett. B* **521** 299 (2001), hep-ph/0108145.
- [29] G. Alimonti *et al.* (Borexino collaboration), hep-ex/0012030.

- [30] P. Alivisatos *et al.* (Kamland collaboration), Stanford-Hep-9803; A. Piepke (Kamland collaboration), in Neutrino 2000.
- [31] J. N. Bahcall, P. I. Krastev and A. Yu. Smirnov, Phys. Rev **D62** 093004 (2000).
- [32] E. Kh. Akhmedov and J. Pulido, hep-ph/0201089.

Experiment	Data	Theory	Data/Theory	Reference
Homestake	$2.56 \pm 0.16 \pm 0.15$	$7.7 \pm 1.3$	$0.332 \pm 0.05$	[1]
Ga	$74.7 \pm 5.13$	$129 \pm 8$	$0.58 \pm 0.06$	[4],[3]
SuperKamiokande	$2.32 \pm 0.085$	$5.05 \pm 1.0$	$0.459 \pm 0.005 \pm 0.016$	[2]
SNO	$1.75 \pm 0.15$	$5.05 \pm 1.0$	$0.347 \pm 0.029$	[19]

Table I - Data from the solar neutrino experiments. Units are SNU for Homestake and Gallium and  $10^6 cm^{-2} s^{-1}$  for SuperKamiokande and SNO. The result for Gallium is the combined one from SAGE and Gallex+GNO.

Fit	$\Delta m_{21}^2 (eV^2)$	$B_0 (G)$	$\chi^2_{rates}/2$ d.o.f.	g.o.f.
1.1	$7.04 \times 10^{-9}$	$4.2 \times 10^4$	2.15	34.1%
1.2	$7.35 \times 10^{-9}$	$6.5 \times 10^4$	2.17	33.8%
1.3	$8.38 \times 10^{-9}$	$1.35 \times 10^5$	1.32	51.7%
1.4	$8.62 \times 10^{-9}$	$1.67 \times 10^5$	1.81	40.4%
1.5	$1.0 \times 10^{-8}$	$2.34 \times 10^5$	1.12	57.1%
2.1	$1.28 \times 10^{-8}$	$9.6 \times 10^4$	1.96	37.6%
2.2	$1.29 \times 10^{-8}$	$1.18 \times 10^5$	2.75	25.3%
2.3	$1.37 \times 10^{-8}$	$1.72 \times 10^5$	1.51	47.1%
2.4	$1.38 \times 10^{-8}$	$1.96 \times 10^5$	2.37	30.6%
2.5	$1.43 \times 10^{-8}$	$2.47 \times 10^5$	1.12	57.3%
2.6	$1.48 \times 10^{-8}$	$2.73 \times 10^5$	2.19	33.5%
2.7	$1.59 \times 10^{-8}$	$3.23 \times 10^5$	0.986	61.1%
3.1	$1.45 \times 10^{-8}$	$1.09 \times 10^5$	1.73	42.2%
3.2	$1.87 \times 10^{-8}$	$1.83 \times 10^5$	2.15	34.1%
4.1	$1.43 \times 10^{-8}$	$9.8 \times 10^4$	1.34	51.2%
4.2	$1.41 \times 10^{-8}$	$1.31 \times 10^5$	3.41	18.2%
4.3	$1.49 \times 10^{-8}$	$2.04 \times 10^5$	1.17	55.8%
4.4	$1.49 \times 10^{-8}$	$2.38 \times 10^5$	2.74	25.4%
4.5	$1.58 \times 10^{-8}$	$3.05 \times 10^5$	1.10	57.8%

Table II - Rate fits: local minima of  $\chi^2_{rates}$  for profiles 1, 2, 3, 4 (eqs.(1)-(13)). Only the fits 1.1, 1.2 (profile 1), 2.1, 2.2 (profile 2), 3.1 (profile 3) and 4.1 (profile 4) are considered for the global analysis (rates + day/night spectrum). The remainder correspond to a value of  $B_0$  largely exceeding  $10^5 G$ . See the text for details.

Fit	$\Delta m_{21}^2 (eV^2)$	$B_0 (G)$	$\chi^2_{gl}/39d.o.f.$	g.o.f.
1.1	$6.80 \times 10^{-9}$	$4.0 \times 10^4$	36.2	59.7%
1.2	$7.07 \times 10^{-9}$	$6.8 \times 10^4$	36.3	59.2%
2.1	$1.27 \times 10^{-8}$	$9.4 \times 10^4$	36.0	60.9%
2.2	$1.26 \times 10^{-8}$	$1.22 \times 10^5$	38.4	49.5%
3.1	$1.41 \times 10^{-8}$	$1.04 \times 10^5$	35.4	63.6%
4.1	$1.45 \times 10^{-8}$	$9.6 \times 10^4$	35.1	64.7%

Table III - Global fits with the three rates (Homestake, Gallium, SNO) and the SuperKamiokande day/night spectrum. Fit 4.1, besides being the best, although by a small margin, is related to a solar field profile which agrees most closely with the requirements from a solar physics analysis (details in the text).

### Figure captions

Fig. 1. Global fits 1.1, 1.2 (lower left, corresponding to profile (1)) and 3.1 (upper right, corresponding to profile 3) and their 95% (dashed) and 99% CL (solid) contours. See also table III.

Fig. 2. Same as fig.1 for global fit 2.1, 2.2 (profile 2). See also table III.

Fig. 3. Same as fig.1 for global fit 4.1 (profile 4). See also table III.

Fig. 4. The theoretical prediction of the SuperKamiokande recoil electron spectrum (solid line) superimposed on the data set [2] (1258 days) for global fit 4.1 (profile 4). This is also the best fit found in the analysis, for which  $\chi^2_{global} = 35.1$  (or g.o.f.=64.7%) for 39 d.o.f..

Fig. 1.

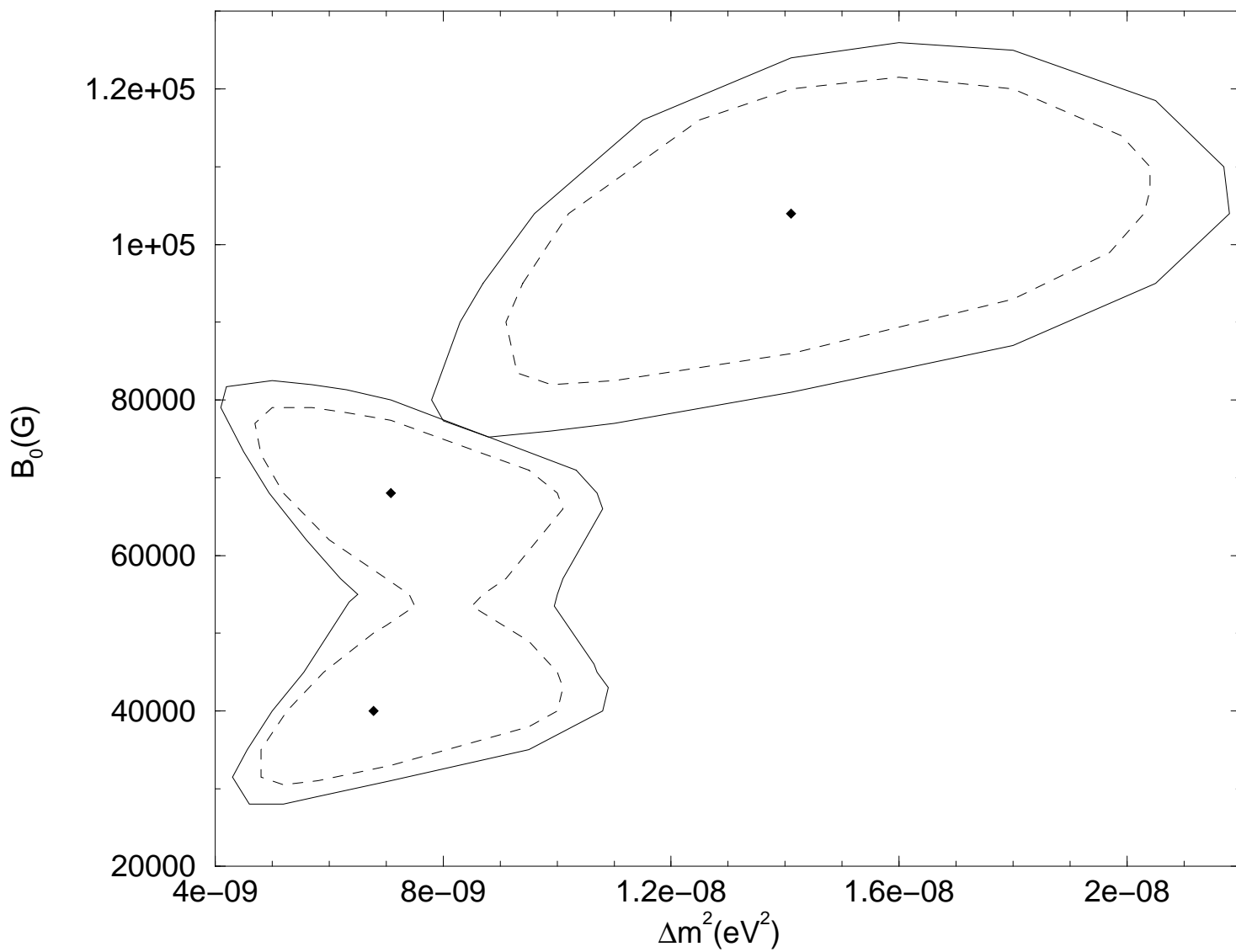


Fig. 2.

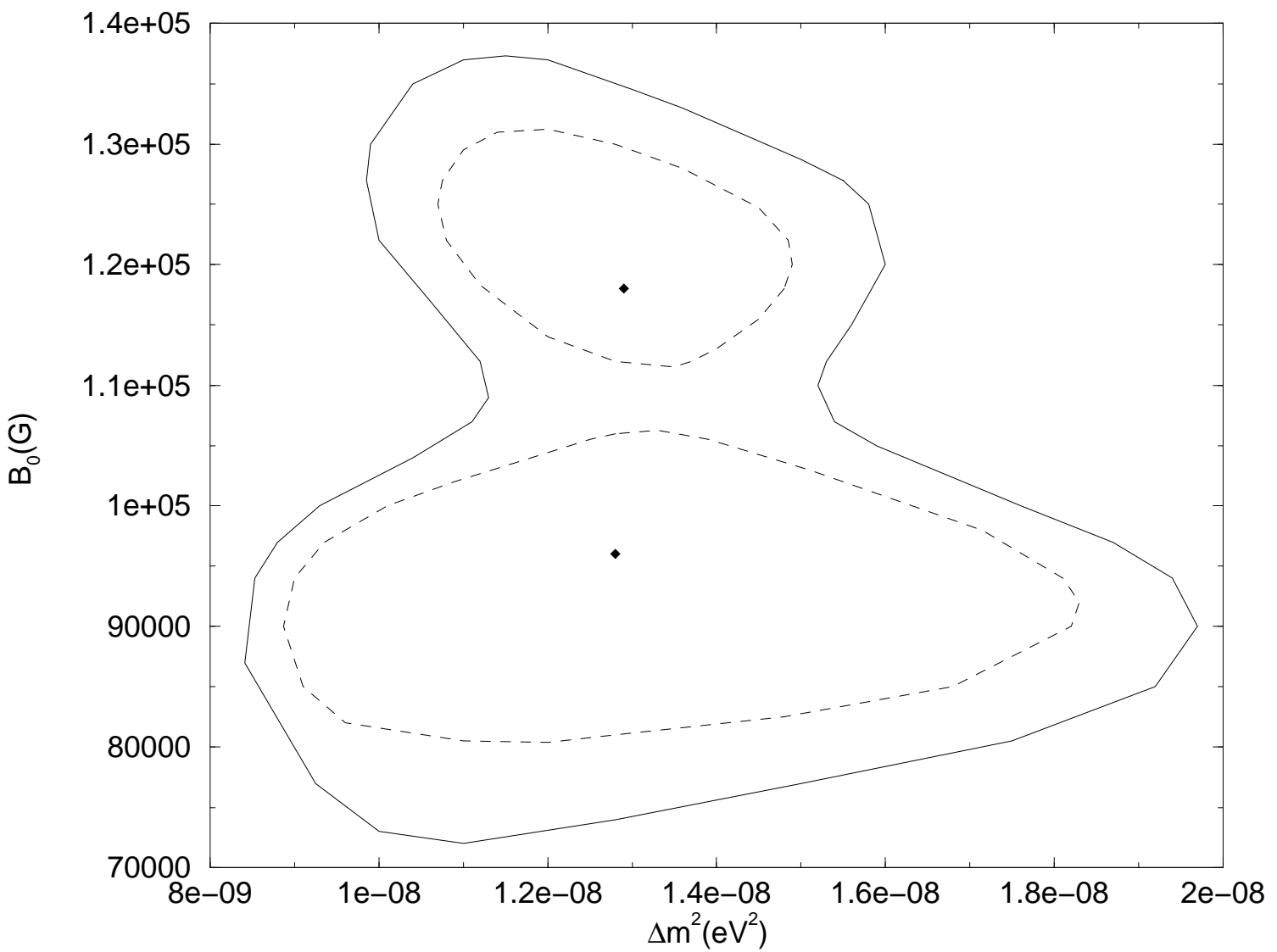


Fig. 3.

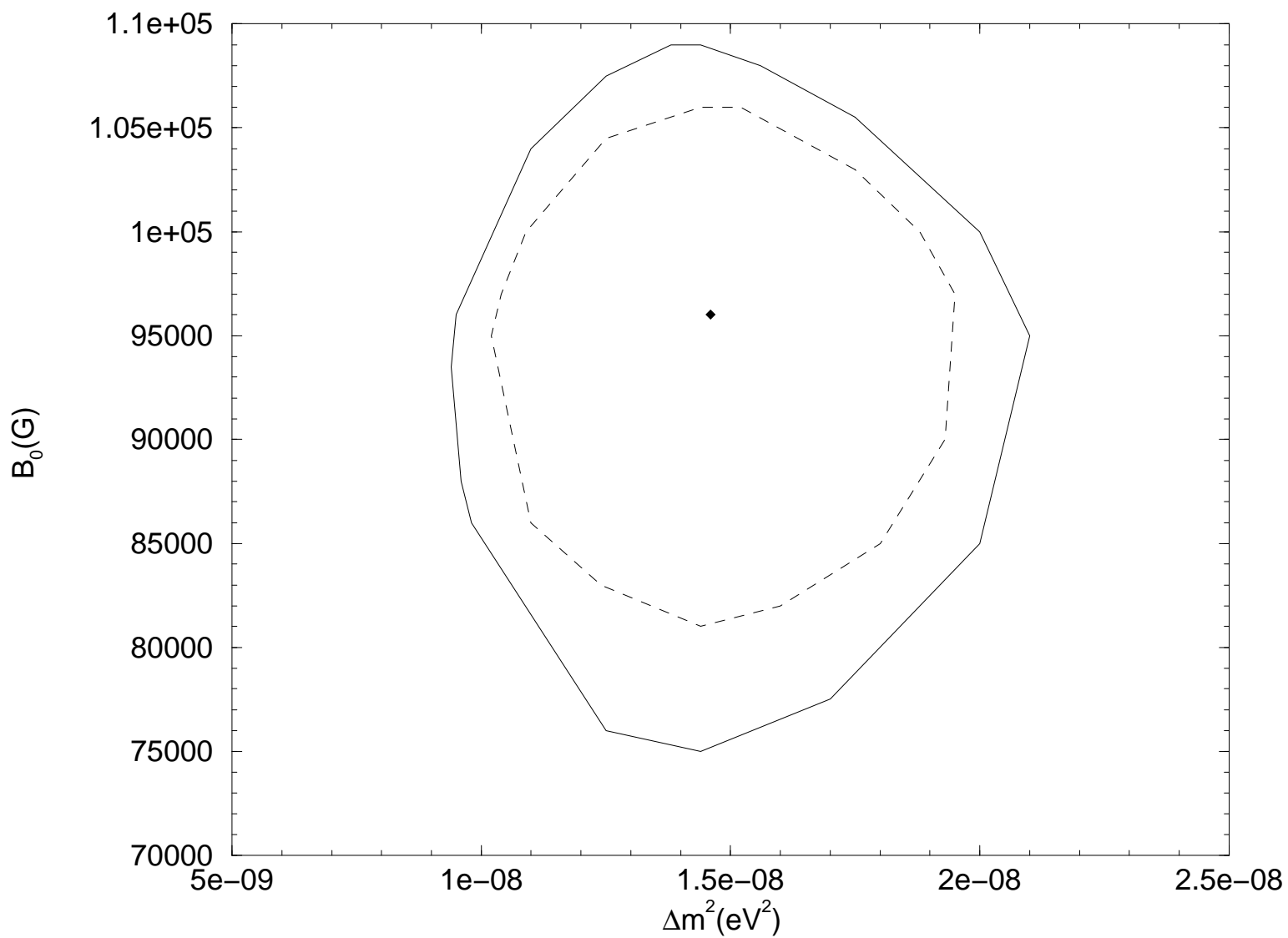


Fig. 4.

